Nanomechanical Heterogeneity in the Gap and Overlap Regions of Type I Collagen Fibrils with Implications for Bone Heterogeneity

Majid Minary-Jolandan and Min-Feng Yu*

Department of Mechanical Science and Engineering, University of Illinois at Urbana−Champaign, 1206 West Green Street, Urbana, Illinois 61801

Received May 6, 2009; Revised Manuscript Received July 22, 2009

The microstructure of type I collagen, consisting of alternating gap and overlap regions with a characteristic *D* period of ∼67 nm, enables multifunctionalities of collagen fibrils in different tissues. Implementing near-surface dynamic and static nanoindentation techniques with atomic force microscope, we reveal mechanical heterogeneity along the axial direction of a single isolated collagen fibril from tendon and show that, within the *D* period, the gap and overlap regions have significantly different elastic and energy dissipation properties, correlating the significantly different molecular structures in these two regions. We further show that such subfibrillar heterogeneity holds in collagen fibrils inside bone and might be intrinsically related to the excellent energy dissipation performance of bone.

Introduction

Type I collagen, as a structural protein, is the most abundant protein in mammals. Collagen fibrils, through formation of biocomposites and modification of hierarchical structures, provide mechanical stability, toughness, and strength in tissues with different mechanical requirements, such as bone, tendon, dentin, skin, and cornea.[1] The diameter of a single collagen fibril varies based on the specific tissues and could be from several tens of nanometers to micrometer range.[2] It is composed of collagen molecules with ∼1.5 nm diameter and ∼300 nm length staggered along the axial direction of the fibril and stabilized by electrostatic and hydrophobic interactions and covalent cross-links.[2−7] Each molecule is displaced in the axial direction by $D \sim 67$ nm with respect to the adjacent molecules. Such a so-called "quarter staggered" structure creates periodic gap (∼0.6*D*) and overlap (∼0.4*D*) regions where the gap region has 20% less packing density than the overlap region (Figure 1a,b). The ability of collagen fibrils to adopt different mechanical properties in different tissues is partly attributed to the different properties of the gap and overlap regions. It is believed that stiff mineral nanocrystals in bone are nucleated specifically in the gap regions.[8,9] Cell membrane integrins (α2, β1 integrins) attach specifically onto the more flexible regions in the collagen fibril in extracellular matrix, providing the structural basis for mechanochemical transduction.[10] Most proteoglycans have a pronounced preference to bind noncovalently but specifically to the gap regions and link fibrils together into an in-registry parallel order in tissues such as tendon.[11−13] Such observations bring about the importance of revealing the different mechanics and chemistry of the gap and overlap regions in collagen fibrils. Previous mechanical studies, such as indentation and bending using atomic force microscopy (AFM)[14−18] and tensile testing using MEMS (microelectromechanical systems)[19] and AFM,[20] however, have mostly aimed only at providing bulk mechanical properties of collagen fibril and have not directly resolved the mechanical heterogeneity in the gap-overlap regions. Heterogeneity in mineralized collagen fibrils and the effect of demineralization have been investigated only recently, using static nanoindentation.[21] Alternatively, X-ray scattering studies of collagen fibrils in their natural state or under tensile deformation have revealed the structure of the gap-overlap regions with ever

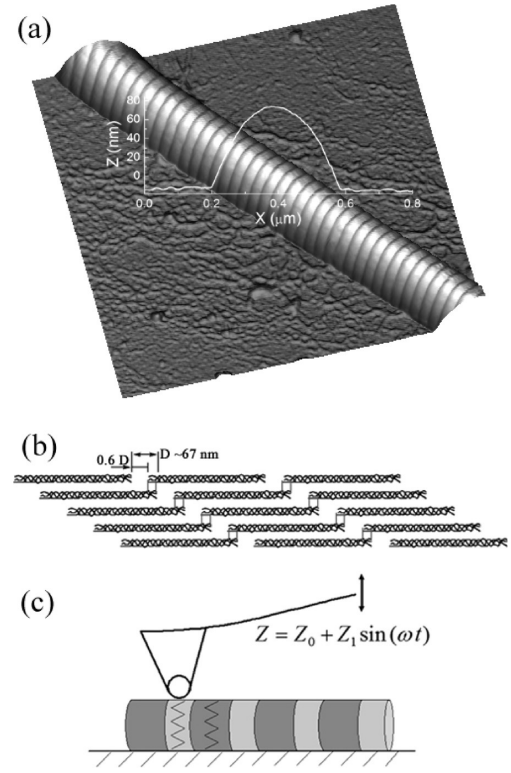

Figure 1. (a) AFM topography image of a collagen fibril of ∼85 nm in diameter. The image scan size is 2 μm. A representative line profile across the fibril is overlaid on the image. (b) Schematic showing the quarter-stagger arrangement of collagen molecules in axial direction of a collagen fibril and the gap-overlap regions as indicated. (c) Schematic showing the experimental arrangement for the dynamic nanoindentation with AFM on a collagen fibril.

* To whom correspondence should be addressed. Tel.: 01-217-333-9246. Fax: 01-217-333-1942. E-mail: mfyu@uiuc.edu.

10.1021/bm900519v CCC: $40.75
Published on Web 08/20/2009

increasing detail, and provided valuable insight into understanding the deformation mechanism of collagen fibrils,[7,22−24] but the quantitative and direct experimental validation of the correlation between the structural and mechanical heterogeneities in collagen fibril has not been fully established.

In this letter, we report the quantitative evaluation of the nanomechanical heterogeneity in the gap and overlap regions of individual type I collagen fibrils with both static and dynamic AFM nanoindentation. Both the continuous mapping with dynamic nanoindentation and the collective sampling with static nanoindentation clearly resolved the significant difference in elastic and energy dissipation properties of the gap and the overlap regions within the *D* period of collagen fibril and, thus, the significant mechanical heterogeneity in collagen fibrils.

Materials and Methods

Sample Preparation. Type I collagen fibrils prepared from bovine Achilles tendon (Sigma-Aldrich) were used. About 10 mg of the extract was mixed with ∼20 mL of 0.01 M sulfuric acid and was stored overnight in refrigerator at below 4 °C. The dispersion was shred by a blender for ∼10 min at 0 °C to produce individual collagen fibrils.[20,25] Different solution concentration was made by adding phosphate buffer saline (PBS). A Si chip cleaned by ethanol and deionized water was dipped into the final solution to collect collagen fibrils on its surface. The Si surface was then rinsed with deionized water several times to wash out the loosely attached collagen fibrils and precipitated salt crystals from the PBS solution. The substrate was then allowed to dry at room temperature. In addition, thin cortical bone samples dissected from animal subjects were prepared for AFM study. The bone samples were first polished by fine sand papers, then partially demineralized by dipping in a diluted phosphoric acid to expose the surface collagen fibrils, and washed several times with PBS buffer.[26]

AFM Characterization. A Dimension 3100 AFM (Veeco Instruments Inc.) equipped with a signal access module, a function generator (Stanford Research System DS 340), a lock-in amplifier (Signal Recovery model 5210), and a data acquisition system (National Instruments) was used for the measurement. Silicon AFM probes (MikroMasch, Inc.) with resonance frequency of ∼75 kHz were used throughout the study. Spring constant of the cantilevers was determined to be ∼4.1 N/m with a thermal noise method.[27] The radius of curvature of the AFM tip was determined to be ∼27 ± 4 nm from imaging a tip calibration sample consisting of ultrasharp spikes (Aurora NanoDevices, Inc.).[29,30] The reverse imaging by the sharp spikes provides a direct topographic mapping of the very end of the AFM tip and from which the shape of the tip end and the tip radius of curvature are obtained. All nanoindentation measurements were carried out in a controlled humidity of under 12% at room temperature by enclosing the AFM scanning system inside a sealed environment regulated with the flow of dry nitrogen gas.

Collagen fibrils were imaged first with the tapping mode AFM to examine the overall quality of their characteristic banding pattern or any structural damages originally existed or induced during the shredding process. After identifying a candidate collagen fibril with high quality along its entire length, the AFM was switched to contact mode to carry out the static and dynamic nanoindentation experiments. No proteoglycan or other protein contents were noticed in our AFM imaging.

Dynamic Nanoindentation with AFM. The dynamic nanoindentation with AFM,[28] similar in principle to the classic dynamic mechanical analysis method for measuring viscoelastic properties of materials,[31] extracts both the elastic and the viscoelastic properties of materials with nanoscale spatial resolution. Here, a small harmonic signal (the drive signal) at a low frequency (<1 kHz) is externally applied onto the z piezo-element in AFM operated in normal contact imaging mode ($Z = Z_0 + Z_1 \sin(\omega t)$; Figure 1c). While the AFM tip is always engaged and a constant force is applied onto the sample surface in the normal contact mode, the drive signal modulates the base movement of the AFM cantilever (so the drive amplitude), and thus modulates the force applied onto the sample surface from the AFM probe. The resulting modulation of the AFM cantilever deflection ($d = d_0 + d_1 \sin(\omega t + \phi)$) contains both the elastic deformation information (in the deflection amplitude of the AFM cantilever, d_1) and the viscoelastic information (in the phase difference between the oscillation of the AFM cantilever and the drive signal, ϕ) of the sample.[32−34] The deflection amplitude and the phase shift were demodulated in real time from the deflection signal with a lock-in technique. The deflection amplitude and the phase shift images were constructed and displayed simultaneously with the contact mode topography image of the studied surface by feeding the demodulated signals back into the AFM system through the available input channels.

A deflection amplitude image reveals variation in elastic property across sample surface. Considering a collagen fibril as an elastic rod with different stiffness in the gap and overlap regions, softer regions in the fibril deform more under the same indentation force from the AFM tip, which in turn means that the deflection amplitude of the AFM cantilever is less under the same drive amplitude. Similarly, a phase shift image shows the difference in viscoelastic property across sample surface.[32−34] Sample regions with larger mechanical damping induce larger phase shift due to the nonlinear viscoelastic behavior in such regions. In our measurement, the drive amplitude and the spring constant of the AFM cantilever were selected to limit the indentation depth to below 2 nm for preventing unintended damage to the fibril surface, and to probe the near surface mechanical properties. The time constant of the lock-in amplifier was set to 10 ms to avoid the signal cross-coupling between the neighboring pixels during the image data acquisition at a scan rate of 0.1 Hz and at a resolution of 256 pixel/line.

Static Nanoindentation with AFM. In static nanoindentation, the AFM tip is positioned on the sample surface and is displaced against the surface, and a nanoindentation curve recording the cantilever deflection (i.e., the indentation force) and tip displacement is acquired. A reference nanoindentation curve is first acquired from a rigid sample (thus assuming not deformable under the tested load) with the AFM probe. For acquiring the indentation curve from a collagen fibril, the AFM tip is engaged on the symmetric surface top of the collagen fibril before the indentation process. In this case, the deformable collagen and the AFM probe act as two springs in series. The net indentation deformation of the collagen is obtained by subtracting the acquired indentation curve from the collagen fibril with the reference nanoindentation curve. In this manner, the force-deformation curve for indentation of collagen fibrils is obtained. We note that in most commercial AFM systems, the probe cantilever makes an angle of ∼10° with the horizon plane and the applied force is nonvertical. The AFM-based nanoindentation method is thus not suitable for quantitative studies involving large indentation deformation. In this study, we limited the maximum indentation below 3 nm and kept the deformation within the elastic regime.

The force-deformation curve is then analyzed using the classical Hertzian contact theory. Hertzian contact theory describes contact of two elastic bodies with corresponding principal radii of curvature at the point of the contact.[35] For a spherical body, two principal radii are the same (R_{sphere}) and for a cylindrical body, one radius of curvature is the radius of the cylinder (R_{cylinder}) and the other is infinity.

AFM probe is modeled as a spherical indenter having a radius of curvature R_{tip}, as previously calibrated. The collagen fibril is modeled as a cylindrical elastic material with its axis parallel to the indentation plane, and its radius R_{collagen} measured from the AFM topography imaging. The indentation deformation δ under an indentation force F is[35]

$$\delta = \frac{3kFK(k')}{2\pi}\left(\frac{A+B}{b/\Delta}\right) \quad (1)$$

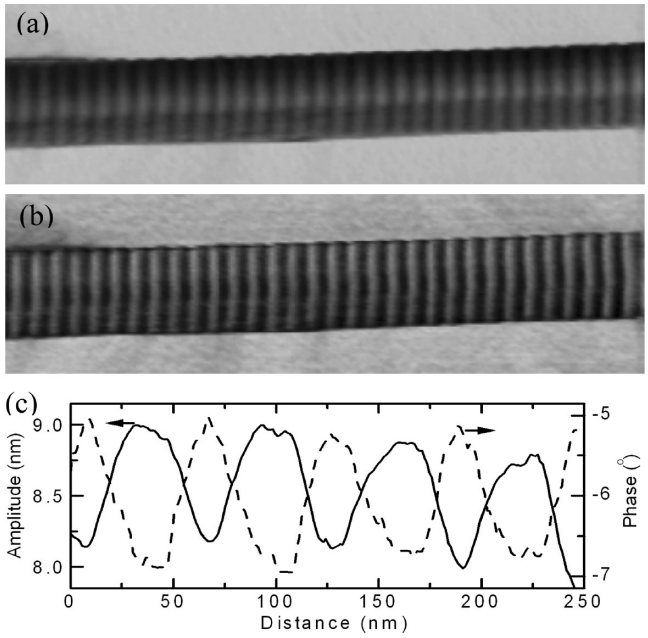

Figure 2. Acquired images showing the deflection amplitude (a) and the phase shift (b) in dynamic nanoindentation along an ~75 nm diameter collagen fibril on a Si substrate, revealing the variation of elastic deformation and the difference in viscoelastic response, respectively. The image is rendered in gray scale with lighter gray representing larger amplitude (so smaller indentation) in (a) and smaller phase shift in (b). The scan size in both images is 2 μm. (c) The corresponding line scans over four D periods showing the deflection amplitude and phase shift variations.

where A and B are constant: $A = 1/2R_{tip}$, $B = 1/2(1/R_{tip} + 1/R_{collagen})$, $\Delta = 1/[(A + B)E^*]$, E^* is the reduced modulus of the sphere and cylinder combination, $1/E^* = (1 - \nu_{tip})/E_{tip} + (1 - \nu_{collagen})/E_{collagen}$, with ν indicating the Poisson's ratio and E the elastic modulus; $K(k')$ and $E(k')$ are the elliptical integrals of the first and second kind, respectively; $k = b/a$, $k' = \sqrt{1 - k^2}$, and a and b are the semimajor and semiminor axis of the ellipse of contact; k' is obtained from solving the nonlinear equation, $B/A = [(1/k^2)E(k') - K(k')]/[K(k') - E(k')]$.

Results and Discussion

Dynamic Nanoindentation of Isolated Collagen Fibrils of Tendon. Figure 1a shows the tapping mode topography of a single isolated collagen fibril with a diameter of ~85 nm on Si substrate. The ~67 nm characteristic banding pattern of gap-overlap regions is apparent in the image. Figure 2 shows the corresponding deflection amplitude and phase shift images acquired from a single collagen fibril rendered in grayscale. In the deflection amplitude image (Figure 2a), the Si surface around the collagen fibril showed, as expected, uniform bright contrast, indicating little indentation deformation, while the collagen fibril was overall in low level gray, with the gap and overlap regions showing different gray levels, meaning reduced deflection amplitude and different elastic deformation in these regions. A line scan obtained from Figure 2a, as shown in Figure 2c, showed more clearly this variation in elastic deformation with the overlap region having larger deflection amplitude and thus being stiffer than the gap region. Similarly, there existed a clear difference in the degree of phase shift in the gap and overlap regions as seen in Figure 2b and in the plot (Figure 2c), suggesting different mechanical damping responses in these regions. (In the phase shift image, lighter gray represents a smaller phase shift.) In average, the overlap region had a larger phase shift (~0.03 rad more) than the gap region, indicating more mechanical damping. The specific identification of the gap and overlap regions in the deflection and phase shift images was made by comparing the images with the topography image acquired simultaneously in the experiment.

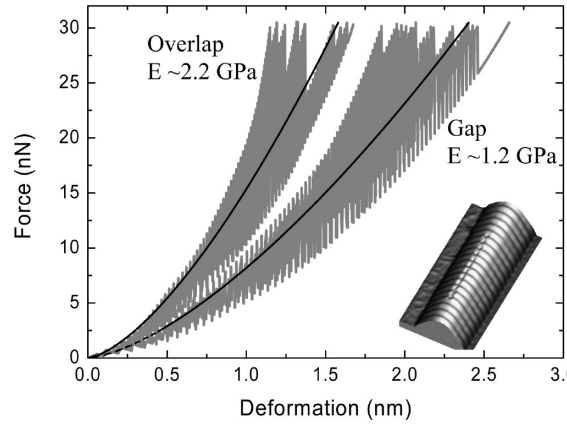

Figure 3. Force−indentation curves acquired from different locations on a ~82 nm diameter collagen fibril with the static AFM nanoindentation. The left and right gray-shaded areas envelop the 13 curves acquired on the overlap region and 15 curves on the gap region, respectively. The black lines in the shaded areas are approximate fits with the Hertzian contact model providing an average elastic modulus ~2.2 GPa for the overlap region and ~1.2 GPa for the gap region. The inset shows the distribution of the indent marks along a surface center line on the studied collagen fibril.

Static Nanoindentation of Isolated Collagen Fibrils of Tendon. To further quantify the mechanical heterogeneity in collagen fibrils, we carried out static nanoindentation measurements at different surface locations along a center line parallel to the long axis of collagen fibrils (an example is shown in the inset in Figure 3). We found that with small forces (<~100 nN) no indentation mark is left on the collagen fibril, which made locating the exact position of the indentation, whether on gap or on overlap region, difficult. To be able to locate the exact indentation spot, we have applied larger forces. However, for extracting the elastic information, we analyze only the initial portion of the force−indentation curve (<30 nN in indentation force and <5% of the fibril diameter in indentation depth). In this indentation range, we found the mechanical deformation in the collagen fibrils being elastic. The exact points of indentation were identified from the residual indentation marks and were categorized into three regions: the overlap region, the gap region, and the boundary region between the gap and overlap regions. The force−indentation curves were then accordingly grouped. The gray areas in Figure 3 show the corresponding envelopes of the force−indentation curves from the 13 measurements on the different overlap regions and the 15 measurements on the different gap regions, respectively. The difference in elastic response in these two regions is evident. To gain a quantitative estimate of this difference, we approximately fitted the response envelops based on the Hertzian contact model with the sample elastic modulus as the only fitting parameter. The fitted curves (the dark lines within the gray areas in Figure 3) provided an elastic modulus of ~2.2 GPa for the overlap region and ~1.2 GPa for the gap region. It is noted that, based on the contact theory, the diameter difference between the overlap and gap regions in the collagen fibril (only about 2−4 nm measured from the acquired AFM topography images) accounts for less than 1% of the measured difference in elasticity between these regions. This static nanoindentation result is in agreement with the result from the previous dynamic

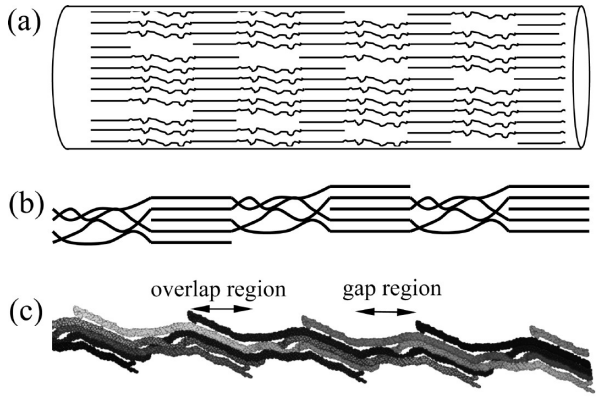

Figure 4. Schematic showing the structural arrangement of the collagen molecules in the gap and overlap regions in a collagen fibril (a) and in a microfibril (b), for example, the common path of the molecules in the overlap region and the rather disorder and kinked molecules in the gap region. (c) The structure of a type I collagen microfibril constructed directly from the X-ray diffraction measurement, adapted from ref 23 with permission.

nanoindentation mapping showing the overlap region being elastically stiffer than the gap region and validates the heterogeneous variation of elasticity along the length of a single collagen fibril. It is also noted that a small variation in tip radius of curvature used for the analysis does not significantly change the obtained elastic moduli. For example, varying the tip radius of curvature from 20 to 35 nm in our contact model analysis changes the elastic moduli from 1.06 to 1.3 GPa and from 2 to 2.48 GPa for the gap and overlap regions, respectively.

Structural Origin of the Subfibrillar Mechanical Heterogeneity. To elucidate the measured difference in elasticity and mechanical damping between the gap and overlap regions, we consider the structural arrangement of collagen molecules within a collagen fibril. A microfibril (~4 nm in diameter) consisting of five quarter-staggered collagen molecules is considered to be the building block of a collagen fibril.[23,36,37] At an ~30 nN indentation force, which is the maximum force in the analysis of the experimental result in our study, the maximum contact area is an ellipse of $\sim 10 \times 20$ nm^2 estimated from the Hertzian contact model, which overlays several microfibrils. Therefore, considering the structural organization of a microfibril is relevant to the interpretation of our experimental data. At the outset, a 20% difference in elasticity is expected due to less packing density by missing one molecule per microfibril in the gap region compared to the overlap region. The packing density alone, however, cannot explain the significant difference in elasticity (~100%) in the gap-overlap regions revealed in our experiment.

Based on the newly resolved X-ray structure of collagen microfibril, it is suggested that collagen molecules are parallel and tightly packed in the overlap region, but form a rather randomly kinked network in the gap region,[7,23] as schematically depicted in Figure 4. As such, each molecule must have several kinked regions.[24] It has also been suggested that such kinks might occur in the gap region of the collagen fibril due to reduced packing density and also lower levels of proline and hydroxyproline.[22] Furthermore, it has been suggested that regions devoid of proline and hydroxyproline are the more flexible regions of the collagen chain, and are predicted to form folds in the collagen molecule that can unfold when stretched.[38−41] The low packing density and the existence of kinks make the gap region understandably softer and more deformable when compared to the overlap region, while in the overlap region the rigid covalent cross-links at two ends of the overlap region[2,3] make the region additionally stiffer. The ~2-fold difference in elastic modulus within the collagen fibril of tendon, however, is still quite significant considering the lack of any previous direct measurements or modeling data. It strongly implies that the existence of various structural folds might be a major factor in determining the overall mechanical stiffness of the gap region.

Due to the finite size of the AFM tip and the expected load transfer through the peptide backbone during the nanoindentation measurement, we could well overestimate the modulus for the softer (gap) region and underestimate the stiffer (overlap) region. The exact difference in mechanical stiffness between the gap and the overlap regions might be larger and the obtained 2-fold difference in relative stiffness is an underestimation.

Another rather interesting result from the study is the observation of higher energy dissipation (or mechanical damping) in the overlap region compared to the gap region, as obtained from dynamic nanoindentation. The result bears two meanings. On the one hand, it means that the gap region, though soft and with kinks, is overall an integral structure responsive elastically to mechanical deformation through its structural network as a whole. On the other hand, there exist certain energy dissipation mechanisms unique to the overlap region that play dominant roles in dynamic deformation. One such mechanism may involve the sliding and friction between collagen molecules. As discussed in other studies, even though the collagen molecules in the overlap region are well aligned and closely packed, they are mostly bonded together by weak electrostatic or hydrophobic interactions except several covalent cross-links near the ends of the overlap region.[5−7] The weak interaction between the close-packed molecules may facilitate breaking and reformation of such weak bonds under oscillatory mechanical deformation in our experiment, allowing augmented energy dissipation in the form of sliding and friction between the molecules.

The deformation and energy dissipation mechanisms revealed in our study is in agreement with what has been postulated for collagen fibrils from previous tensile deformation studies of tendon. Such studies have suggested that three deformation modes may have been involved in a collagen fibril under tension, namely, molecular elongation through direct stretch of the molecules, increase of the length of the gap regions, and the relative sliding between adjacent molecules.[42−44] Experiments have indeed found that only 10% of the applied macroscopic strain on tendon causes direct stretching of collagen molecules and the rest 90% of the strain is accommodated by fibrillar and molecular slippage.[38,42] More specifically, it has been suggested that the heel region in the stress−strain curve acquired from the synchrotron X-ray diffraction based tensile test of tendon tissue may be due to the straightening of molecular kinks in the gap regions.[22,24]

Containing alternating soft and stiff regions gives collagen fibrils enormous flexibility in adapting themselves to different requirements in mechanical strength and toughness in different tissues. The structure resembles spring-dashpot pairs in series with different spring constants and dashpot coefficients. Under ordinary mechanical load, the gap region would mostly accommodate the deformation through the extension and retraction of the kinks, hence, would translate little to the direct stretching of collagen molecules. Such hierarchy and heterogeneity mediate passing of smaller fractions of mechanical strain to lower levels, and hence increase the durability of the impacted tissue. For example, one of the major functions of tendon is to transmit and store energy produced by muscle, which would require the

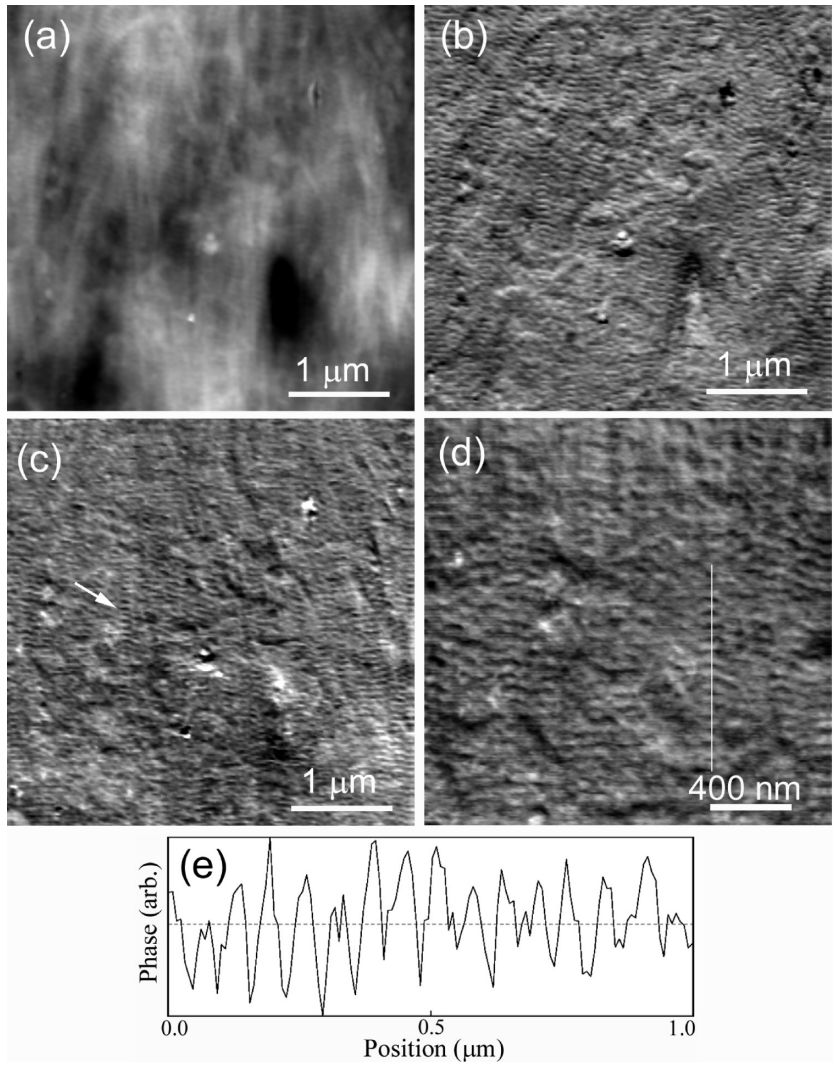

Figure 5. AFM dynamic nanoindentation mapping of a bone sample surface showing the topography image (a), the dynamic nanoindentation amplitude image (b), and the dynamic nanoindentation phase image (c) of the same region in the bone sample. A smaller scan size phase image (d) around the region marked with an arrow in (c) reveals better the individual collagen fibrils in bone and the mechanical heterogeneity within. A line profile (e) over a collagen fibril marked in (d) shows the periodic variation of the mechanical damping capacity with a period of ~67 nm.

reversible stretching of collagen fibrils with sufficient mechanical durability.[45]

Subfibrillar Mechanical Heterogeneity of Collagen Fibrils in Bone. Another implication of this hierarchical and heterogeneous structure in collagen fibril can be seen in bone mineralization. It is reported that stiff apatite crystals (~100 GPa) tend to deposit in the gap region[8,9] to increase its stiffness, which in turn increases the overall stiffness of the collagen fibril without sacrificing the toughness regulated by the energy dissipation mechanisms.[46,47] It has been further proposed that nanoscale heterogeneity promotes energy dissipation in bone.[48] We have performed a dynamic nanoindentation mapping on a thin cortical bone surface partially demineralized to reveal the surface collagen fibrils according to the reported procedure.[26,49] Surface maps revealing the elastic stiffness difference and the mechanical damping difference across the bone surface were obtained as shown in Figure 5, including the difference within even individual collagen fibrils. A similar map has been obtained on a dentin sample with the use of nanoindenter, although in that study individual collagen fibrils were not resolved.[50] As shown in Figure 5b,c and more clearly in Figure 5d, the mechanical heterogeneity revealed previously within isolated single collagen fibrils of tendon persisted for the fibrils in bone. This indicates that the lowest level of hierarchy in terms of mechanical heterogeneity in bone and tendon might be the subfibrillar structure in each single collagen fibril. We are currently performing a more quantitative mechanical analysis of bone samples with different degrees of mineralization. It is hypothesized that the coexistence of hard mineral nanocrystals and subfibrillar mechanical heterogeneity of collagen would extend the mechanical hierarchy in bone right down to the nanoscale.[51]

In this study, air-dried collagen fibrils and bone samples were used to avoid the complications that may arise due to the presence of water. It has been shown, as expected, that upon drying the elastic modulus of the collagen fibrils increases.[14] Therefore, the value of elastic modulus reported here is not indicative of that of collagen in vivo. However, the mechanical heterogeneity observed in such dry samples is intrinsic to the structural organization of the collagen fibrils and is expected to mostly remain even in samples at physiological conditions. Different structural models are also proposed for collagen fibrils including the core−shell model where a collagen fibril is considered to be consisted of a softer core and a harder shell.[52]

However, we have only analyzed the small indentation properties of the collagen fibrils, and hence, our results are restricted to represent only the near-surface properties of such fibrils.

Conclusion

By its structural organization, with aligned molecules in the axial direction, a type I collagen is generally understood to be an anisotropic material. Using near surface static and dynamic nanoindentation measurements with AFM, we revealed that a collagen fibril isolated from a bovine Achilles tendon was, in addition, heterogeneous along its axial direction in terms of its mechanical properties (elastic and mechanical damping properties) as a result of the periodic variation of the gap and overlap regions. We further revealed that such subfibrillar mechanical heterogeneity was maintained within the collagen fibrils exposed on a cortical bone sample surface. More specifically, we found that within a collagen fibril from the tendon the overlap region was elastically stiffer (almost ~100% stiffer) than the gap region, while in the meantime showed higher mechanical damping than the gap region. We reasoned that such mechanical heterogeneity was originated from the uniquely different molecular arrangement in the gap and overlap regions in a collagen fibril and might be responsible for facilitating its multifunctional role in extracellular matrix as well as promoting energy dissipation and toughness in bone. Understanding more detailed mechanical properties of this highly important protein is expected to help in designing better biofunctional scaffolds and finding better treatment of related diseases in the future.

Acknowledgment. We would like to thank Professor Iwona M. Jasiuk of the University of Illinois for providing bone samples. The work is supported by NSF Grants CMMI 0600583 and CBET 0731096.

References and Notes

(1) Fratzl, P. Collagen: Structure and Mechanics, an Introduction. In *Collagen, Structure and Mechanics*; Springer: New York, 2008.
(2) Wess, T. J. Collagen fibrillar structure and hierarchies. *Collagen, Structure and Mechanics*; Springer: New York, 2008.
(3) Hay, E. D. *Cell Biology of Extracellular Matrix*; Plenum Press: New York, 1991.
(4) Lodish, H.; Berk, A.; Matsudaira, P.; Kaiser, C. A.; Krieger, M.; Scott, M. P.; Zipursky, S. L.; Darnell, J. *Mol. Cell. Biol.*; Freeman, New York, 2004.
(5) Hulmes, D. J. S.; Miller, A.; Parry, D. A. D.; Piez, K. A.; Woodhead-Galloway, J. *J. Mol. Biol.* **1973**, *79*, 137–148.
(6) Itoh, T.; Kobayashi, M.; Hashimoto, M. *Jpn. J. Appl. Phys.* **1998**, *37*, L190–L192.
(7) Orgel, J. P. R. O.; Miller, A.; Irving, T. C.; Fischetti, R. F.; Hammersley, A. P.; Wess, T. J. *Structure* **2000**, *9*, 1061–1069.
(8) Weiner, S.; Wagner, H. D. *Annu. Rev. Mater. Sci.* **1998**, *28*, 271–298.
(9) Robinson, R. A.; Watson, M. L. *Anat. Rec.* **1952**, *114*, 383–409.
(10) Silver, F. H.; DeVore, D.; Siperko, L. M. *J. Appl. Physiol.* **2003**, *95*, 2134–2141.
(11) Hedlund, H.; Mengarelli-Widholm, S.; Heinegard, D.; Reinholt, F. P.; Svensson, O. *Matrix Biol.* **1994**, *14*, 227–232.
(12) Scott, J. E. *J. Physiol.* **2003**, *553*, 335–434.
(13) Raspanti, M.; Alessandrini, A.; Ottani, V.; Ruggeri, A. *J. Struct. Biol.* **1997**, *119*, 118–122.
(14) Wenger, M. P. E.; Bozec, L.; Horton, M. A.; Mesquida, P. *Biophys. J.* **2007**, *93*, 1255–1263.
(15) Yang, L.; van der Werf, K. O.; Fitie, C. F. C.; Bennink, M. L.; Dijkstra, P. J.; Feijen, J. *Biophys. J.* **2008**, *94*, 2204–2211.
(16) Heim, A. J.; Matthews, W. G.; Koob, T. J. *Appl. Phys. Lett.* **2006**, *89*, 181902–18904.
(17) Heim, A. J.; Koob, T. J.; Matthews, W. G. *Biomacromolecules* **2007**, *8*, 3298–3301.
(18) Grant, A. C.; Brockwell, D. J.; Radford, S. E.; Thomson, N. H. *Appl. Phys. Lett.* **2008**, *92*, 233902–233904.
(19) Shen, Z. L.; Dodge, M. R.; Kahn, H.; Ballarini, R.; Eppell, S. J. *Biophys. J.* **2008**, *95*, 3956–3963.
(20) van der Rijt, J. A. J.; van der Werf, K. O.; Bennink, M. L.; Dijkstra, P. J.; Feijen, J. *Macromol. Biosci.* **2006**, *6*, 697–702.
(21) Balooch, M.; Habelitz, S.; Kinney, J. H.; Marshall, S. J.; Marshall, G. W. *J. Struct. Biol.* **2008**, *162*, 404–410.
(22) Fratzl, P.; Misof, K.; Zizak, I.; Rapp, G.; Amenitsch, H.; Bernstorff, S. *J. Struct. Biol.* **1997**, *122*, 119–122.
(23) Orgel, J. P. R. O.; Irving, T. C.; Miller, A.; Wess, T. J. *Proc. Natl. Acad. Sci. U.S.A.* **2006**, *103*, 9001–9005.
(24) Mosif, K.; Rapp, G.; Fratzl, P. *Biophys. J.* **1997**, *72*, 1376–1381.
(25) Minary-Jolandan, M.; Yu, M.-F. *Nanotechnology* **2009**, *20*, 085706.
(26) Tai, K.; Qi, H. J.; Ortiz, C. *J. Mater. Sci.: Mater. Med.* **2005**, *16*, 947–959.
(27) Butt, H. J.; Jaschke, M. *Nanotechnology* **1995**, *6*, 1–7.
(28) Maivald, P.; Butt, H. J.; Gould, S. A. C.; Prater, C. B.; Drake, B.; Gurley, J. A.; Elings, V. B.; Hansma, P. K. *Nanotechnology* **1991**, *2*, 103–106.
(29) Westra, K. L.; Thomson, D. J. *J. Vac. Sci. Technol., B* **1994**, *12*, 3176–3181.
(30) Westra, K. L.; Mitchell, A. W.; Thomson, D. J. *J. Appl. Phys.* **1993**, *74*, 3608–3610.
(31) Menard, K. P. *Dynamic Mechanical Analysis: A Practical Introduction*; CRC Press: Boca Raton, FL, 1999.
(32) Radmacher, M.; Tillman, R. W.; Gaub, E. H. *Biophys. J.* **1993**, *64*, 735–742.
(33) Minary-Jolandan, M.; Yu, M.-F. *Ultramicroscopy* **2008**, *108*, 821–526.
(34) Mahaffy, R. E.; Shih, C. K.; MacKintosh, F. C.; Kas, J. *Phys. Rev. Lett.* **2000**, *85*, 880–883.
(35) Boresi, A. P. *Advanced Mechanics of Materials*; John Wiley & Sons: New York, 1993.
(36) Baselt, D. R.; Revel, J. P.; Baldeschwieler, J. D. *Biophys. J.* **1993**, *65*, 2644–2655.
(37) Holmes, D. F.; Gilpin, C. J.; Baldock, C.; Ziese, U.; Koster, A. J.; Kadler, K. E. *Proc. Natl. Acad. Sci. U.S.A.* **2001**, *98*, 7307–7312.
(38) Silver, F. H.; Freeman, J. W.; Horvath, I.; Landis, W. J. *Biomacromolecules* **2001**, *2*, 750–756.
(39) Landis, W. J.; Silver, F. H.; Freeman, J. W. *J. Mater. Chem.* **2006**, *16*, 1495–1503.
(40) Silver, F. H.; Horvath, I.; Foran, D. J. *J. Theor. Biol.* **2002**, *216*, 243–254.
(41) Paterlini, M. G.; Nemethy, G.; Scheraga, H. A. *Biopolymers* **2004**, *35*, 607–619.
(42) Mosler, E.; Folkhard, W.; Knörzer, E.; Nemetschek-Gansler, H.; Nemetschek, Th.; Koch., M. H. J. *J. Mol. Biol.* **1985**, *182*, 589–596.
(43) Folkhard, W.; Mosler, E.; Geercken, W.; Knörzer, E.; Nemetschek-Gansler, H.; Nemetschek, Th.; Koch, M. H. J. *Int. J. Biol. Macromol.* **1987**, *9*, 169–175.
(44) Sasaki, N.; Odajima, S. *J. Biomech.* **1996**, *29*, 1131–1136.
(45) Walsh, W. R. *Repair and Regeneration of Ligaments, Tendons and Joint Capsule*; Humana Press: Totowa, NJ, 2006.
(46) Fratzl, P.; Gupta, H. S.; Paschalis, E. P.; Roschger, P. *J. Mater. Chem.* **2004**, *14*, 2115–2123.
(47) Gupta, H. S. Nanoscale deformation mechanisms in collagen. *Collagen, Structure and Mechanics*; Springer: New York, 2008.
(48) Tai, K.; Dao, M.; Suresh, S.; Palazoglu, A.; Ortiz, C. *Nat. Mater.* **2007**, *6*, 454–462.
(49) Hassenkam, T.; Fantner, G. E.; Cutroni, J. A.; Weaver, J. C.; Morse, D. E.; Hansma, P. K. *Bone* **2004**, *35*, 4–10.
(50) Balooch, G.; Marshall, G. W.; Marshall, S. J.; Warren, O. L.; Asif, S. A. S.; Balooch, M. *J. Biomech.* **2004**, *37*, 1223–1232.
(51) Currey, J. *J. Musculoskeletal Neuronal Interact.* **2005**, *5*, 317.
(52) Gutsman, T.; Fantner, G. E.; Venturoni, M.; Ekani-Nkodo, A.; Thompson, J. B.; Kindt, J. H.; Morse, D. E.; Fygenson, D. K.; Hansma, P. K. *Biophys. J.* **2003**, *84*, 2593–2598.

BM900519V